Title

Optimization of pyrazole-containing 1,2,4-triazolo-[3,4-b]thiadiazines, a new class of STAT3 pathway inhibitors

Journal

Bioorganic & Medicinal Chemistry Letters, 26(15)

ISSN

0960-894X

Authors

LaPorte, Matthew G
Wang, Zhuzhu
Colombo, Raffaele
et al.

Publication Date

2016-08-01

DOI

10.1016/j.bmcl.2016.06.017

Peer reviewed

HHS Public Access

Author manuscript

Bioorg Med Chem Lett. Author manuscript; available in PMC 2017 August 01.

Published in final edited form as:

Bioorg Med Chem Lett. 2016 August 1; 26(15): 3581–3585. doi:10.1016/j.bmcl.2016.06.017.

Optimization of pyrazole-containing 1,2,4-triazolo-[3,4-*b*]thiadiazines, a new class of STAT3 pathway inhibitors

Matthew G. LaPorte[a], **Zhuzhu Wang**[a,b], **Raffaele Colombo**[a], **Atefeh Garzan**[a], **Vsevolod A. Peshkov**[a], **Mary Liang**[a,b], **Paul A. Johnston**[b,c], **Mark E. Schurdak**[c,d], **Malabika Sen**[e], **Daniel P. Camarco**[b], **Yun Hua**[b], **Netanya I. Pollock**[e], **John S. Lazo**[f], **Jennifer R. Grandis**[g], **Peter Wipf**[a,b,c,d], and **Donna M. Huryn**[a,b]

[a]University of Pittsburgh Chemical Diversity Center, University of Pittsburgh, Pittsburgh, Pennsylvania 15260, USA

[b]Department of Pharmaceutical Sciences, University of Pittsburgh, Pittsburgh, Pennsylvania 15261, USA

[c]University of Pittsburgh Cancer Institute, Pittsburgh, Pennsylvania 15260, USA

[d]University of Pittsburgh Drug Discovery Institute, University of Pittsburgh, Pittsburgh, Pennsylvania 15260, USA

[e]Department of Otolaryngology, University of Pittsburgh, Pittsburgh, Pennsylvania 15260, USA

[f]Department of Pharmacology, University of Virginia, Charlottesville, Virginia 22908, USA

[g]Department of Otolaryngology-Head and Neck Surgery, University of California, San Francisco, California 94158, USA

Abstract

Structure-activity relationship studies of a 1,2,4-triazolo-[3,4-*b*]thiadiazine scaffold, identified in an HTS campaign for selective STAT3 pathway inhibitors, determined that a pyrazole group and specific aryl substitution on the thiadiazine were necessary for activity. Improvements in potency and metabolic stability were accomplished by the introduction of an α-methyl group on the thiadiazine. Optimized compounds exhibited anti-proliferative activity, reduction of phosphorylated STAT3 levels and effects on STAT3 target genes. These compounds represent a starting point for further drug discovery efforts targeting the STAT3 pathway.

Graphical Abstract

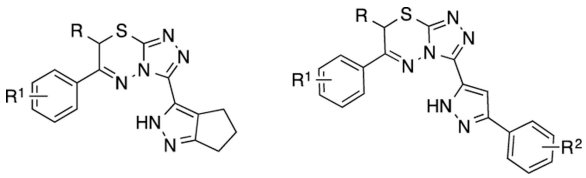

Keywords

STAT3 inhibitor; Triazolo-thiadiazines; Anti-cancer agents; STAT1

While advancements in detection and treatment have aided in the longstanding campaign against cancer, new annual U.S. cancer cases and related deaths still exceed 1.5 million and 580,000, respectively.[1] Recently, new therapies have targeted signaling pathways that are aberrantly activated in transformed cells. These pathways promote cancer cell survival and proliferation, but they play a less important role in normal cell survival.[2] As a part of our interest in the development of mechanism-based anticancer agents,[3,4] we have been pursuing novel small molecule inhibitors of the signal transducer and activation of transcription 3 (STAT3) pathway.[5,6,7] STAT3 is a transcription factor that influences many of the acquired capabilities of cancer tumorigenesis, thereby making it an attractive target for the development of oncolytics.[8–12]

There is mounting evidence for its role in cancer such as increased levels of activated STAT3 (*p*STAT3-Y705) observed in many cancers including head and neck squamous cell carcinomas (HNSCC).[4,5] We previously reported the use of a high content phenotypic screen to identify selective inhibitors of the STAT3 activation pathway compared to STAT1 which served as an important selectivity control since the latter is a tumor-suppressive transcription factor.[6,7] We identified several scaffolds that met this criteria. Herein, we describe the optimization and structure activity relationship for a series of pyrazole-containing 1,2,4-triazolo-[3,4-*b*]thiadiazines with selective STAT3 pathway inhibition.

The high content phenotypic screen, which utilized an interleukin-6 (IL-6)-induced STAT3 activation assay in Cal33 head and neck tumor cells, identified several triazolo-thiadiazines as selective STAT3 pathway inhibitors (e.g., **1a** and **2b**, Table 1).[7] The biological activities of these structurally similar analogs were confirmed through resynthesis and re-assay (*vide infra*). These HTS/HCS hits had no effect on interferon-γ (IFN-γ)-induced STAT1 pathway activation at concentrations up to 50 μM. This selectivity was not observed for many other STAT3 pathway inhibitors reported in the literature including the pan-Janus kinase (JAK) inhibitor, pyridone 6.[6] Furthermore, this series exhibited acceptable drug-like properties: low molecular weight (<400), clogP values between 3 and 4,[13] and anti-proliferative activities with several HNSCC cell lines (GI_{50} 14–45 μM with 686LN, Cal33, FaDu, and OSC19).

Triazolothiadiazines exhibit an array of pharmacological effects including anti-proliferative activities.[14] However, the HTS library included a number of inactive analogs of **1a** and **2b** where the pyrazole was replaced with an alkyl, aryl, or alternative heterocyclic substituents (Figure 1). This suggested that we were not observing broadly promiscuous effects with this scaffold. These observations together with the desirable biological selectivity profile and

favorable drug-like physical properties encouraged us to pursue a medicinal chemistry optimization effort for this series.

The synthesis of **1a** and **2b** required key amino-triazole intermediates **3a** and **3b** that were readily assembled according to literature procedures.[15–19] Alkylations with the appropriate α-halo ketone and microwave-assisted cyclodehydrations afforded the original hits **1a** and **2b** (Scheme 1).

In addition to **1a** and **2b**, two sub-libraries of triazolothiadiazines that maintained either the fused cyclopentyl-pyrazole group ("**a**") or the pendant phenyl-pyrazole group ("**b**") with diversified R-group modifications on the triazolothiadiazine were synthesized. These compounds were prepared according to Scheme 1 with yields ranging from 24–90% by using a variety of α-halo ketones in the final microwave-assisted cyclodehydration reaction. A protected aldehyde derivative was used to prepare **9a** and **9b**.

We selected substituents with diverse steric, polarity, and electronic characteristics. Table 2 illustrates a representative subset of these analogs and their activities in STAT3 and STAT1 assays. The R-substitution on the thiadiazine influenced activities by a factor of greater than 10 with many modifications leading to a loss of STAT3 potency. The importance of the chlorine substitution on the arene groups was evident by the significant drop in activity seen with the removal of the halogen regardless of the pyrazole scaffold (**5a** vs. **1a**; **5b** vs. **2b)**. As a general trend, hydrogen (**9**), aliphatic (**10, 11**), and heterocyclic (**7**) R-groups were inactive regardless of the pyrazole substructure. One notable exception was the chlorothiophene analog **8a** that maintained comparable potency to the initial hit. However, when the chlorothiophene was combined with the phenyl-pyrazole ("**b**") scaffold, the loss of activity of analog **8b** was consistent with other heterocyclic derivatives.

A few SAR trends diverged between the two pyrazole scaffolds. For example, exchanging the R-substituents of **1a** and **2b** provided analogs **1b** and **2a** that were 3–4 times less active. The reduced STAT3 potency of compounds **2a** (26 μM) and **4a** (21 μM) established the importance of the *ortho*- and *para*-chlorine atoms on the phenyl ring in **1a**. Interestingly, the phenyl-pyrazole with the same *meta*-chlorophenyl R-substituent (**4b**) retained, or perhaps, improved the STAT3 potency compared to the *para*-chlorophenyl **2a**, suggesting that either lipophilicity or electronic effects were important. However, the potent activity of the *para*-methoxyphenyl analog **6b** did not support a purely electronic contribution. The selective inhibition of STAT3 over STAT1 activation was maintained within this entire subseries.

To evaluate the effect of thiadiazine modifications, hydrazone **6a** was converted to dihydrothiadiazines **12** and **13** (Scheme 2). Both analogs were inactive in the STAT3 assay, which established the requirement for an unsaturated ring system.

The modified pyrazole analogs shown in Figure 2 were prepared according to Scheme 1.[15] The *para*-chloro and *para*-fluoro substitutions on the 3-arylpyrazoles were well tolerated. The *para*-fluoro analog **14** exhibited an IC_{50} of 7.5 μM, which was a ~4-fold improvement in STAT3 potency over the unsubstituted analog **1b**.[20] In the fused pyrazole "**a**" series, the cyclohexyl homolog **16** was ~2-fold less active than the cyclopentyl analog **1a**.

Despite the favorable biological profiles for some of these compounds, they exhibited poor metabolic stability [**1a**: $t_{1/2}$=14 min in human liver microsomes (HLM); 4 min in mouse liver microsomes (MLM)]. Predictions of metabolic sites using SMARTCyp[21] pointed toward the thioether as the most susceptible site of a cytochrome P450-mediated oxidation (see Supporting Information). Subsequent analysis determined that oxidized thioethers were inactive (*vide infra*).

Analysis of the HTS SAR data suggested that carbon and oxygen heterocyclic analogs of the triazolothiadiazines would be inactive despite their potential to be more metabolically stable. Therefore, in an effort to address this possible metabolic liability, we designed, prepared and tested a series of analogs that were modified at the position alpha to the sulfur atom with the aim of sterically blocking oxidation of the thioether (Scheme 3 and Table 3). These compounds were prepared by microwave-mediated cyclodehydration with the corresponding α-halo ketones and amino-triazoles. All of the final products maintained desirable physical properties such as MW and clogP (Table 3 & Supporting Information). The structure of **17** (UPCDC10263) was confirmed by X-ray analysis (Figure 3).

It was apparent from this series that alkyl substitution alpha to the sulfur atom consistently led to potent inhibition of STAT3 activation while maintaining high selectivity over STAT1. The size of the alkyl groups did not seem to influence potency since large groups, such as *i*-Bu (**25** and **26**) and *i*-Pr (**23** and **24**), were as potent or perhaps slightly more potent than the methyl analogs (**17–22**). The benzyl analog **27** was less active, but only one example was prepared and we cannot speculate whether this was a general trend. In contrast, alkyl groups with polar substituents (**28** and **29**) and *gem*-dimethyl substitution (**30**) were either significantly less potent or inactive in the STAT3 assay. Compounds **28** and **29** exhibited potent anti-proliferative activity in the absence of STAT3 inhibition that is presumed to be due to off-target effects. We prepared the sulfoxide analog of compound **21** (not shown) as the putative oxidative metabolite; however, the resultant compound was inactive.

In some cases, combining the α-methyl substitution with the 3-arylpyrazole scaffold (**19, 20**, and **21**) yielded a 2–3 fold improvement in STAT3 potency compared to the original hit **2b** (Table 3). Chiral separation (Supporting Information) provided individual enantiomers of **22** (*ent*-**1** and *ent*-**2**), and a 3-fold difference in STAT3 potency was observed between these enantiomers. While these differences were not dramatic, the trend suggested the existence of a eutomer [**22** (*ent*-**1**), configuration not assigned] and a distomer within this series. Interestingly, the eudismic ratio was even larger when considering the anti-proliferative activity, which may reflect additional differences in metabolism or transport between the enantiomers (Table 3). Importantly, effects of α-methyl substitutions on microsomal stability were also evident. By incorporating this substitution, we were indeed able to increase the metabolic stability of compound **19** in HLM and MLM ($t_{1/2}$ = 27 min and 10 min, respectively), thereby doubling the stability compared to our initial hits. Some analogs containing alkyl groups larger than methyl (e.g. **23–26**) exhibited low micromolar potency but suffered from reduced compound solubility (data not shown) which excluded them from further characterization. Anti-proliferative activity in Cal33 cells was also determined. In most cases, compounds that inhibited STAT3 also inhibited the growth of HNSCC cell lines (Table 4). However, direct correlations between the two activities are likely complicated by

differences between assay conditions, distinct genetic alterations among the HNSCC cell lines, and/or differences between a compound's metabolic stability, residence time, and transport.[22]

With these encouraging cell-based results in well-characterized HNSCC models, we evaluated the effects of compounds **19** (UPCDC10131) and **22** (UPCDC10205) on STAT3 expression levels by Western blot analysis (Figures 4 and 5). Consistent with the pSTAT3 HCS assay, pronounced decreases in pSTAT3 levels were observed, and both compounds exhibited significant inhibition of the downstream STAT3 target gene, Cyclin D1.[23]

In summary, we identified pyrazole-linked 1,2,4-triazolo-[3,4-*b*]thiadiazines as a new class of potent and selective STAT3 pathway inhibitors. Optimized compounds exhibited anti-proliferative activity, reduction of phosphorylated STAT3 levels, and reduction of downstream effects on STAT3 gene expression targets. Structure-activity relationships established that a pyrazole group and specific aryl substitution on the thiadiazine were required for activity. Significant improvements in potency and metabolic stability were realized through α-substitution of the thiadiazine heterocycle. Further studies of the mechanism of action of these compounds will be reported in due course.

Supplementary Material

Refer to Web version on PubMed Central for supplementary material.

Acknowledgments

The authors would like to thank Dr. Steven J. Geib (University of Pittsburgh) for the X-ray analysis of **17**, and Mr. Peter G. Chambers (University of Pittsburgh) for LCMS/ELS analyses. We are grateful to Christina Kraml (Lotus Separations) for kindly performing chiral separation of **22**. We would also like to thank Lynn O. Resnick for her contributions especially during the early hit-triage and design phase. The authors also appreciate efforts and thoughtful discussions by project team members including Shelby M. Anderson (UPCDC), Erin Skoda (UPCDC), Courtney Vowell (UPCDC), Gabriela Mustata Wilson (UPCDC), Joanne I. Yeh (Univ. Pittsburgh), Xiang-Qun Xie (UPCDC), Kyaw Z. Myint (UPCDC), Qi Xu (UPCDC), Lin Fu (UPCDC), Lirong Wang (UPCDC), Seia Comsa (UPDDI), Albert H. Gough (UPDDI), Tongying Shun (UPDDI), David Zaidins (UPDDI), Neal Green (Leidos Biomedical Research), William J. Moore (Leidos), Shizuko Sei (Leidos), Beverly A. Teicher (NCI), Dianne L. Newton (NCI), Myrtle Davis-Millin (NCI), Joel Morris (NCI), Andy Stephen (NCI). This project was funded in part with federal funds from the National Cancer Institute, National Institutes of Health, under Chemical Biology Consortium Contract No. HSN261200800001E.

References and notes

1. Siegel R, Ma H, Zou Z, Jemal A. Cancer Statistics, 2014. CA Cancer J. Clin. 2014; 64:9. [PubMed: 24399786]
2. Levitzki A, Klein S. Signal transduction therapy of cancer. Mol. Aspects Med. 2010; 31:287. [PubMed: 20451549]
3. See, for example, Alverez C, Arkin MR, Bulfer SL, Colombo R, Kovaliov M, LaPorte MG, Lim C, Liang M, Moore WJ, Neitz RJ, Yan Y, Yue Z, Huryn DM, Wipf P. Structure–activity study of bioisosteric trifluoromethyl and pentafluorosulfanyl indole inhibitors of the AAA ATPase p97. ACS Med. Chem. Lett. 2015; 6:1225. [PubMed: 26713109]
4. Alverez C, Bulfer SL, Chakrasali R, Chimenti MS, Deshaies RJ, Green N, Kelly MM, LaPorte MG, Lewis TS, Liang M, Moore WJ, Neitz RJ, Peshkov V, Walters M, Zhang FZ, Arkin MR, Wipf P, Arkin DM. Allosteric indole amide inhibitors of p97: Identification of a novel probe of the ubiquitin pathway. ACS Med. Chem. Lett. 2016; 7:182. [PubMed: 26985295]

5. LaPorte MG, da Paz Lima DJ, Zhang F, Sen M, Grandis JR, Camarco D, Hua Y, Johnston PA, Lazo JS, Resnick LO, Wipf P, Huryn DM. 2-Guanidinoquinazolines as new inhibitors of the STAT3 pathway. Bioorg. Med. Chem. Lett. 2014; 24:5081. [PubMed: 25288188]
6. Johnston PA, Sen M, Hua Y, Camarco D, Shun TY, Lazo JS, Grandis JR. High-content pSTAT3/1 Imaging Assays to Screen for Selective Inhibitors of STAT3 Pathway Activation in Head and Neck Cancer Cell Lines. Assay Drug Dev. Technol. 2014; 12:55. [PubMed: 24127660]
7. Johnston PA, Sen M, Hua Y, Camarco D, Shun TY, Lazo JS, Wilson GM, Resnick LO, LaPorte MG, Wipf P, Huryn DM, Grandis JR. HCS Campaign to Identify Selective Inhibitors of IL-6-Induced STAT3 Pathway Activation in Head and Neck Cancer Cell Lines. Assay Drug Dev. Technol. 2015; 13:356. [PubMed: 26317883]
8. Hanahan D, Weinberg RA. Hallmarks of Cancer: The Next Generation. Cell. 2011; 144:646. [PubMed: 21376230]
9. Frank DA. STAT3 as a central mediator of neoplastic cellular transformation. Cancer Lett. 2007; 251:199. [PubMed: 17129668]
10. Johnston PA, Grandis JR. STAT3 Signaling: Anticancer Strategies and Challenges. Mol. Interventions. 2011; 11:18.
11. Leeman RJ, Lui VWY, Grandis JR. STAT3 as a therapeutic target in head and neck cancer. Exp. Opin. Biol. Ther. 2006; 6:231.
12. For recent reviews of STAT3 inhibitors, see: Xiong A, Yang Z, Shen Y, Zhou J, Shen Q. Transcription Factor STAT3 as a Novel Molecular Target for Cancer Prevention. Cancers. 2014; 6:926. [PubMed: 24743778] Debnath B, Xu S, Neamati N. Small Molecule Inhibitors of Signal Transducer and Activator of Transcription 3 (Stat3) Protein. J. Med. Chem. 2012; 55:6645. [PubMed: 22650325] Peyser ND, Grandis JR. Critical analysis of the potential for targeting STAT3 in human malignancy. Onco Targets Ther. 2013; 55:999. [PubMed: 23935373] Wake MS, Watson CJ. STAT3 the oncogene – still eluding therapy? FEBS J. 2015; 282:2600. [PubMed: 25825152] Wang X, Crowe PJ, Goldstein D, Yang J-L. STAT3 inhibition, a novel approach to enhancing targeted therapy in human cancers (Review). Int. J. Oncol. 2012; 41:1181. [PubMed: 22842992] Siveen KS, Sikka S, Surana R, Dai X, Zhang J, Kumar AP, Tan BKH, Sethi G, Bishayee A. Targeting the STAT3 signaling pathway in cancer: Role of synthetic and natural inhibitors. Biochim. Biophys. Acta. 2014; 1845:136. [PubMed: 24388873] Furtek SL, Backos DS, Matheson CJ, Reigan P. Strategies and Approaches of Targeting STAT3 for Cancer Treatment. ACS Chem. Biol. 2016; 11:308. [PubMed: 26730496]
13. Physicochemical properties were calculated using: Instant J Chem 5.3.8. Chem Axon. 2010 (http://www.chemaxon.com).
14. (a) Kamel MM, Abdo NYM. Synthesis of novel 1,2,4-triazoles, triazolothiadiazines and triazolothiadiazoles as potential anticancer agents. Eur. J. Med. Chem. 2014; 86:75. [PubMed: 25147148] (b) Khan I, Ibrar A, Zaib S, Ahmad S, Furtmann N, Hameed S, Simpson J, Bajorath J, Iqbal J. Active compounds from a diverse library of triazolothiadiazole and triazolothiadiazine scaffolds: Synthesis, crystal structure determination, cytotoxicity, cholinesterase inhibitory activity, and binding mode analysis. Bioorg. Med. Chem. 2014; 22:6163. [PubMed: 25257911]
15. Wu D, Jin F, Lu W, Zhu J, Li C, Wang W, Tang Y, Jiang H, Huang J, Liu G, Li J. Synthesis, Structure-Activity Relationship, and Pharmacophore Modeling Studies of Pyrazole-3-Carbohydrazone Derivatives as Dipeptidyl Peptidase IV Inhibitors. Chem. Biol. Drug. Des. 2012; 79:897. [PubMed: 22381062]
16. Roy AK, Batra S. Facile Baylis-Hillman Reation of Substituted 3-Isoxazole-carbaldehydes: The Impact of a Proximal Heteroatom Within a Heterocycle on the Acceleration of the Reaction. Synthesis. 2003:2325.
17. Reid JR, Heindel ND. Improved Syntheses of 5-Substituted-4-amino-3-mercapto-(4*H*)-1,2,4-triazoles. J. Heterocycl. Chem. 1976; 13:925.
18. Cai, SX.; Zhang, H-Z.; Kemnitzer, WE.; Drewe, JA.; Sirisoma, NS. 3-Aryl-6-aryl-7*H*-[1,2,4]triazolo]3,4-*b*][1,3,4]thia-diazines and analogs as activators of caspases and inducers of apoptosis and the use thereof. WO. 2009/094205.
19. Dhiman AM, Wadodkar KN, Patil SD. Synthesis and antimicrobial activity of some bridgehead nitrogen heterocycles. Indian J. Chem., Sect. B. 2001; 40B:640.

20. The amino triazole building blocks required for **14–16** (and related analogs) were purchased from commercial sources.

21. (a) Rydberg P, Rostkowski M, Gloriam DE, Olsen L. The Contribution of Atom Accessibility to Site of Metabolism Models for Cytochromes P450. Mol. Pharm. 2013; 10:1216. [PubMed: 23339440] (b) Rydberg P, Gloriam DE, Zaretzki J, Breneman C, Olsen L. SMARTCyp: A 2D Method for Prediction of Cytochrome P450-Mediated Drug Metabolism. ACS Med. Chem. Lett. 2010; 1:96. [PubMed: 24936230]

22. Additional mechanism of action studies will be reported in due course.

23. Leslie K, Lang C, Devgan G, Azare J, Berishaj M, Gerald W, Kim YB, Paz K, Darnell JE, Albanese C, Sakamaki T, Pestell R, Bromberg J. Cyclin D1 Is Transcriptionally Regulated by and Required for Transformation by Activated Signal Transducer and Activator of Transcription 3. Cancer Res. 2006; 66:2544. [PubMed: 16510571]

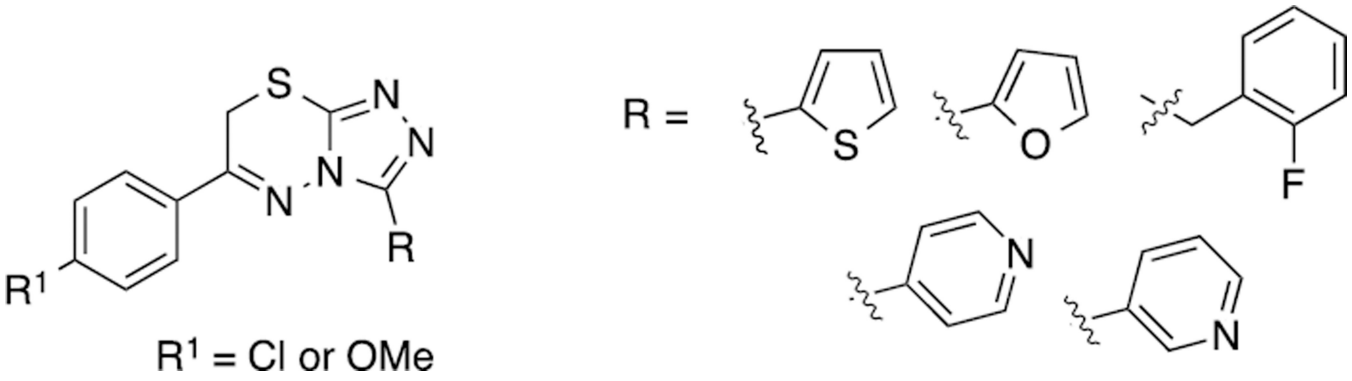

Figure 1.
Inactive Triazolothiadiazines (STAT3 IC_{50} > 50 μM).

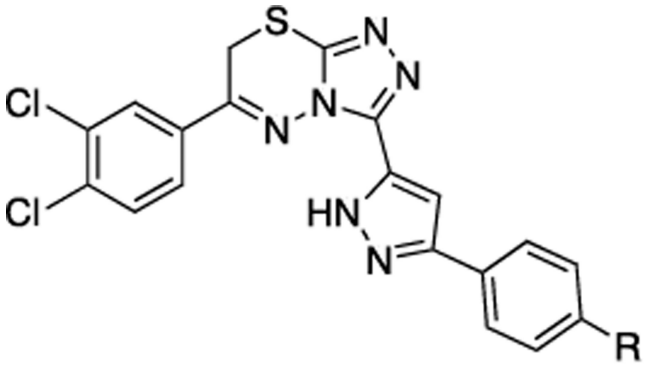

14: R = F; STAT3 IC_{50} = 7.5 ± 2.6 μM
15: R = Cl; STAT3 IC_{50} = 14.5 μM*

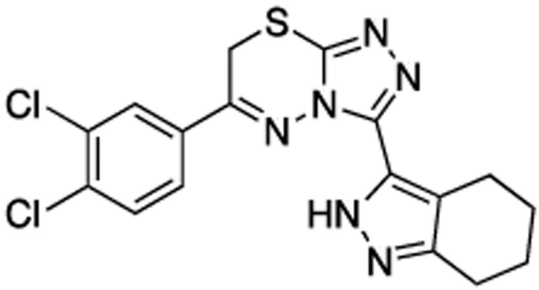

16: STAT3 IC_{50} = 15.5 ± 4.7 μM

Figure 2.
Modified pyrazole analogs (*mean IC_{50}, n=2).

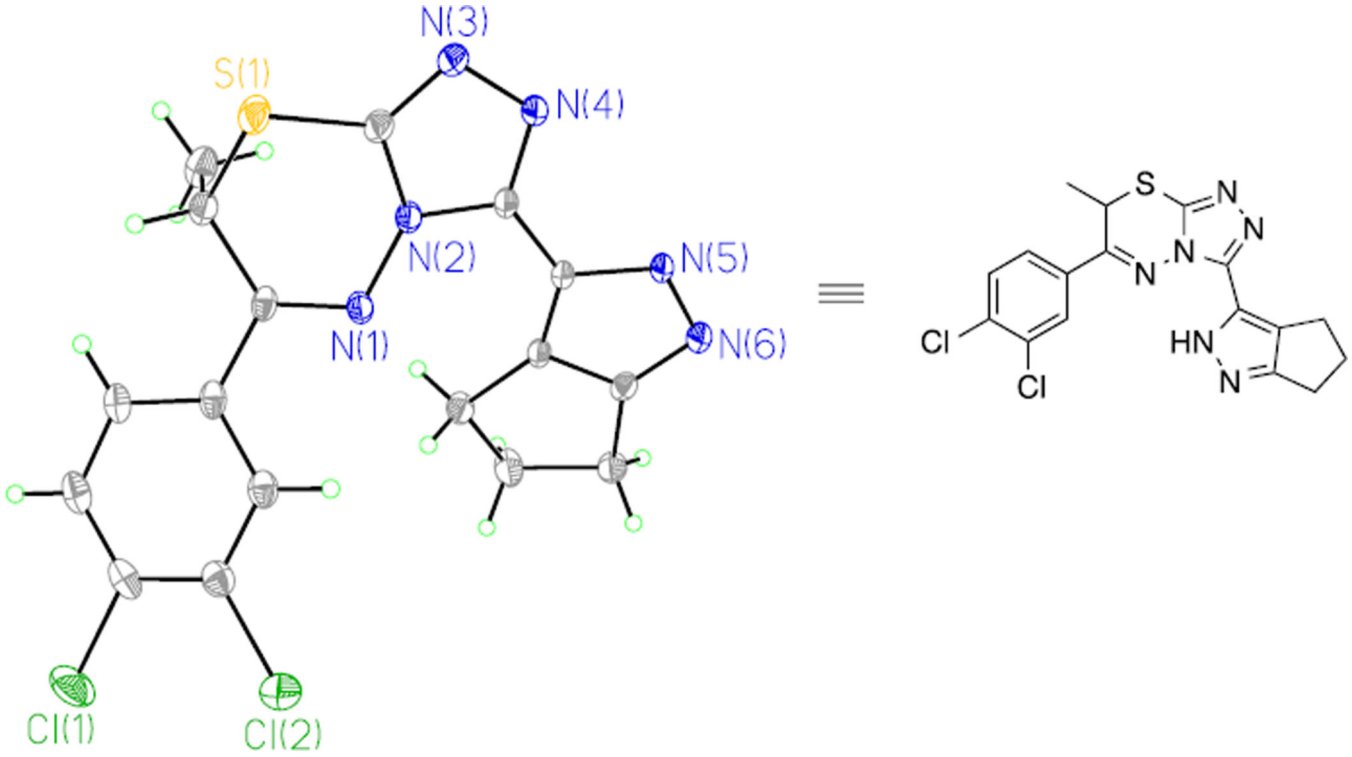

Figure 3.
X-ray structure of Compound **17** (UPCDC10263, CCDC 1481994).

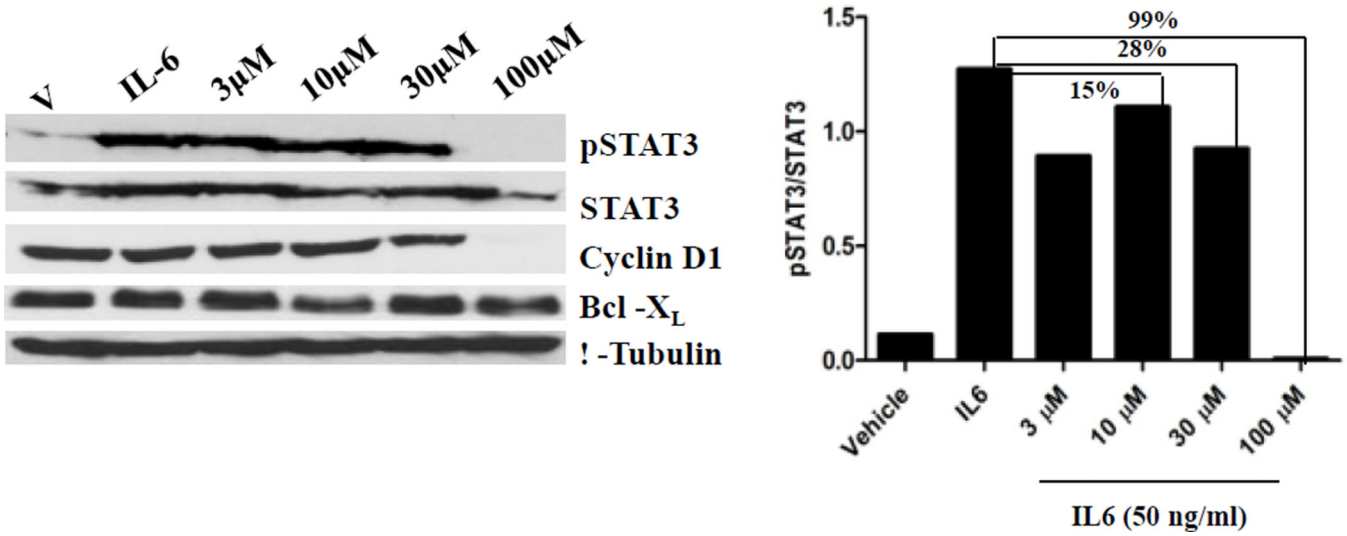

Figure 4.

Western blot analysis of **19** (UPCDC10131) in interleukin 6 (IL-6, 50 ng/mL)-stimulated Cal33 cells.

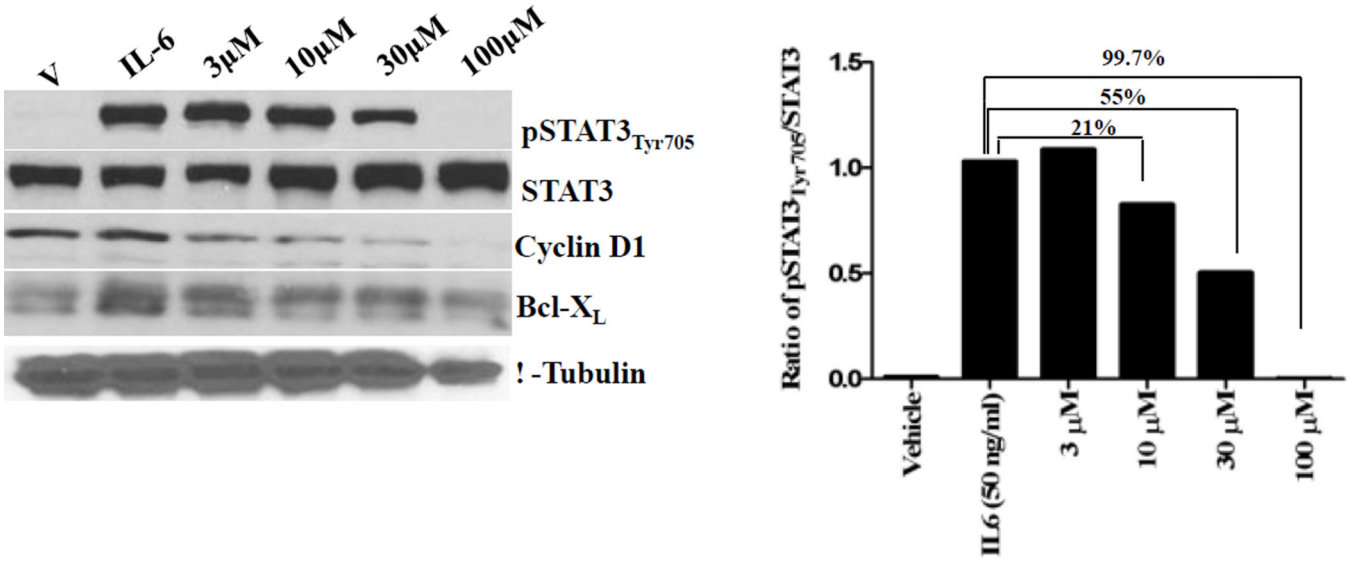

Figure 5.

Western blot analysis of **22** (UPCDC10205) in interleukin 6 (IL-6, 50 ng/mL)-stimulated Cal33 cells.

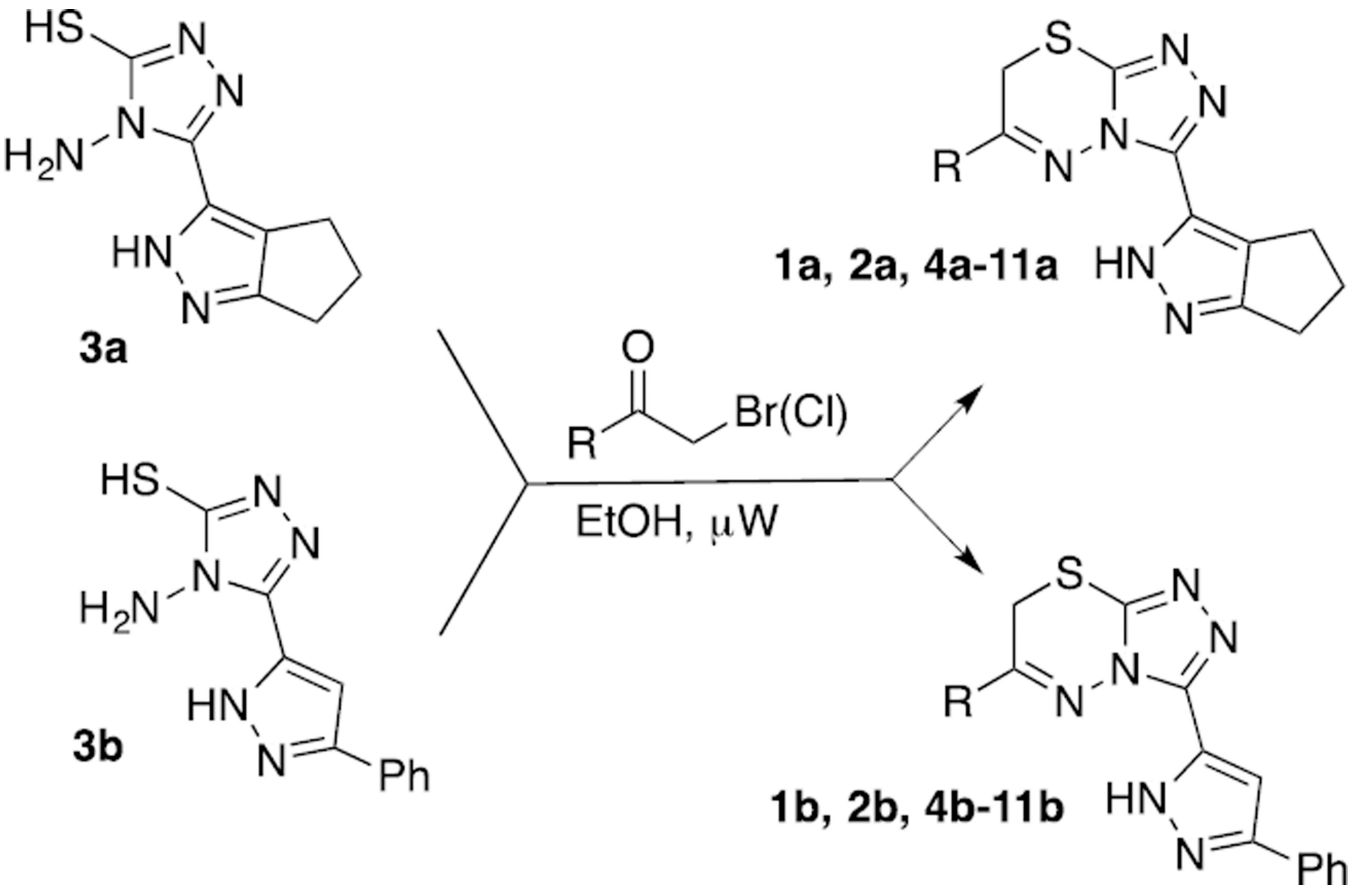

Scheme 1.
Preparation of 1,2,4-triazolo-[3,4-*b*]thiadiazines.

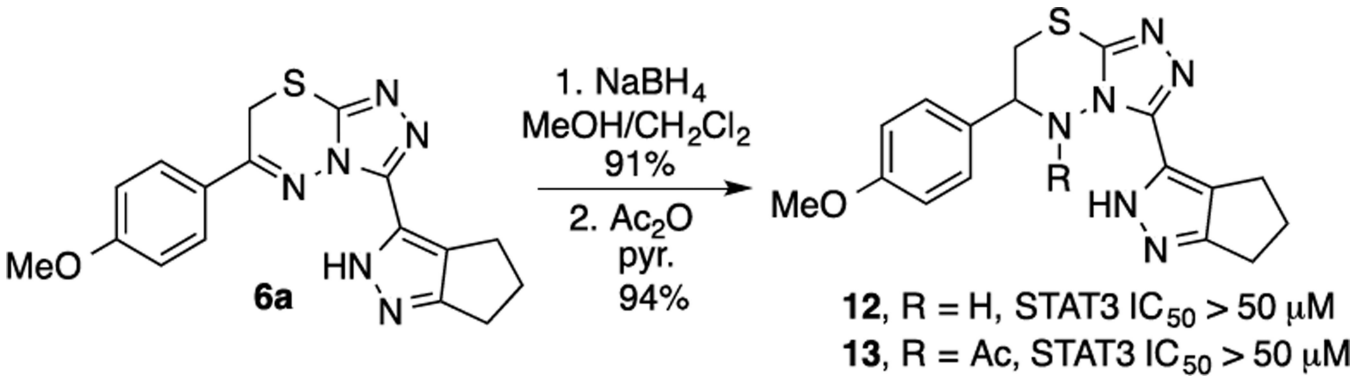

Scheme 2.
Synthesis of dihydrothiadiazine analogs.

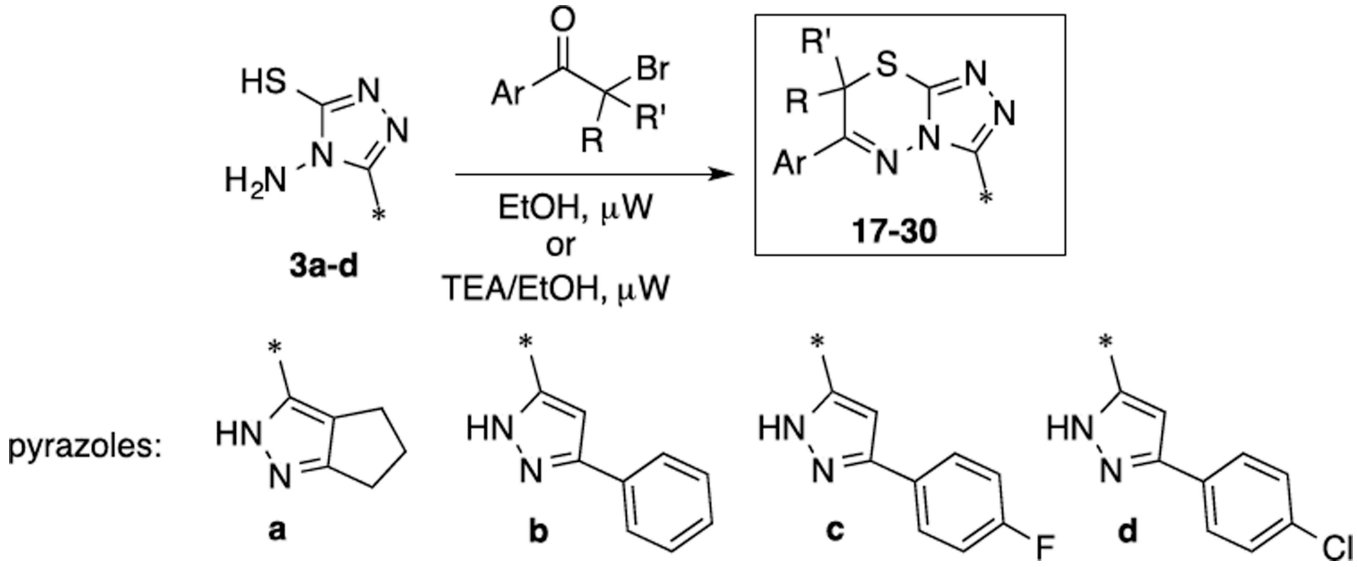

Scheme 3.

Preparation of α-substituted analogs of the thioether moiety.

Table 1

Triazolothiadiazines **1a** and **2b** and Summary of Biological Activities and Physicochemical Properties.

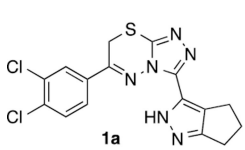

1a

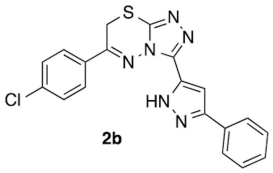

2b

Cmpd #	**1a**	**2b**
STAT3 IC_{50} (μM)	6.8 ± 3.7	9.6 ± 7.8
STAT1 IC_{50} (μM)	> 50	> 50
GI_{50} HNSCC[a] (μM)	14–26	27–44
MW	391.2	392.8
cLogP	3.2	3.7
HBD/HBA	1/4	1/4
tPSA	71.7	71.7
LE	0.29	0.26

[a]Cell lines: 686LN, FaDu, Cal33, OSC19

Table 2

STAT3 and STAT1 activities of triazolothiadiazines. (**a**: cyclopentyl-pyrazole series; **b**: 3-phenyl-pyrazole series)

R	Cmpd #	STAT3 IC_{50} (μM)	STAT1 IC_{50} (μM)
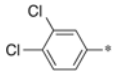	**1a**	6.8 ± 3.7	>50
	1b	31.2 ± 20.0	>50
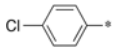	**2a**	26.8 ± 22.3	>50
	2b	9.6 ± 7.8	>50
	**4a**	21.2 ± 5.9	>50
	4b	5.6 ± 4.0	45.9 ± 8.3
	**5a**	21.2 ± 23.5	>50
	5b	27.0 ± 17.4	> 50
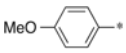	**6a**	17.9 ± 22.9	40.6 ± 7.5
	6b	3.7 ± 2.5	> 50
	**7a**	> 50	> 50
	7b	> 50	> 50
	**8a**	11.0 ± 5.5	> 50
	8b	> 50	> 50
H –*	**9a**	> 50	> 50
	9b	> 50	> 50
Me –*	**10a**	> 50	> 50
	10b	> 50	> 50
	**11a**	> 30	> 50
	11b	> 50	> 50

Table 3

STAT3 and STAT1 activities of α-substituted thioether analogs.

Cmpd #	Pyrazole series	Ar	R/R'	STAT3 IC_{50} (μM)	STAT1 IC_{50} (μM)	Cal33 GI_{50} (μM)
17	a	3,4-dichloro-Ph	Me/H	8.2 ± 2.2	>50	1.9 ± 1.2
18	a	4-OMe-Ph	Me/H	9.1*	>50	0.2*
19	b	Ph	Me/H	3.4*	15*	34.1 ± 8.7
20	c	Ph	Me/H	3.8 ± 0.8	>30	36.3 ± 9.7
21	c	4-OMe-Ph	Me/H	4.2*	>30*	29.5 ± 6.5
22	d	4-OMe-Ph	Me/H	11.4 ± 10.4	29.5*	2.2 ± 0.3
22 (ent-1)	d	4-OMe-Ph	Me/H	5.72*	NT	2.7*
22 (ent-2)	d	4-OMe-Ph	Me/H	17.3*	NT	21.8*
23	a	3,4-dichloro-Ph	*i*-Pr/H	4.4*	>50	8.2*
24	a	4-OMe-Ph	*i*-Pr/H	2.2 ± 1.2	>50	0.4 ± 0.1
25	a	3,4-dichloro-Ph	*i*-Bu/H	4.1*	>50	3.5 ± 1.5
26	b	4-OMe-Ph	*i*-Bu/H	5.1*	>50	0.5*
27	a	3,4-dichloro-Ph	Bn/H	7.5*	>50	3.3*
28	b	4-OMe-Ph	$(CH_2)_2NH_2$/H	>20	NT	2.5*
29	b	4-OMe-Ph	$(CH_2)_2$OMe/H	>50	NT	0.04*
30	a	3,4-dichloro-Ph	Me/Me	18.6*	>50	>50*

*mean IC_{50}, n=2.

Table 4

Growth inhibition on HNSCC cell lines

	18 UPCDC10262	**19 UPCDC10131**	**22 UPCDC10205**
686LN GI_{50} (μM)	0.88 *	32.2 *	17.4 *
Cal33 GI_{50} (μM)	0.18 *	34.1 *	2.2 *
FaDu GI_{50} (μM)	1.3 *	32.7 *	8.4 *
OSC19 GI_{50} (μM)	3.1 *	31.3 *	14.9 *

* mean, n=2